

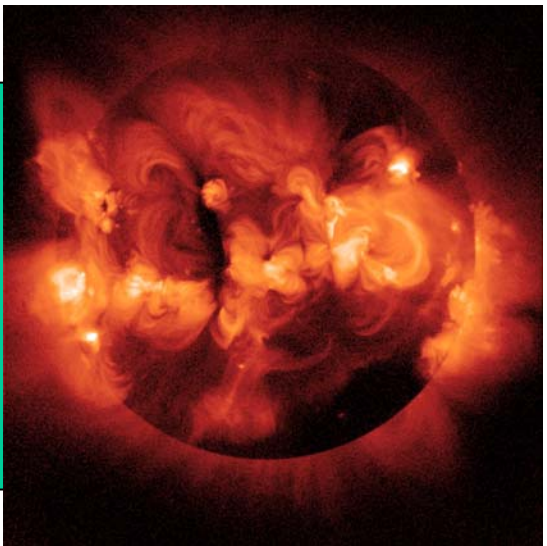
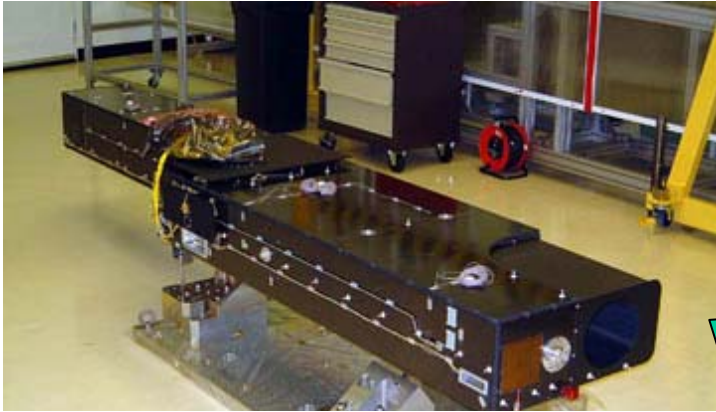
# *Solar and LHD (Large Helical Device) Plasma Diagnostics in EUV*

Tetsuya Watanabe (NAO/NINS)

Takako Kato, Izumi Murakami (NIFS/NINS)

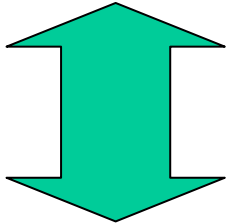
Norimasa Yamamoto (Nagoya U.)

# Solar Coronal Spectra (Time Dep.)

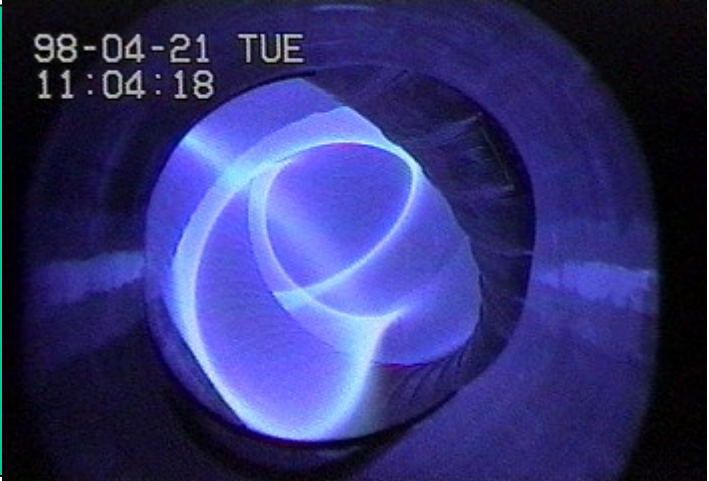
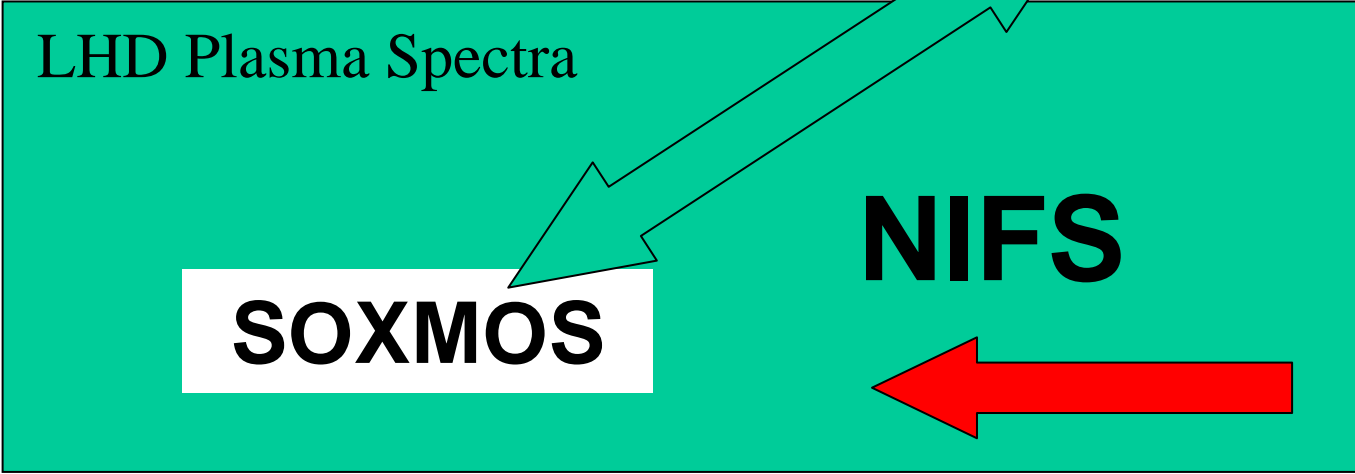


Coronal Plasma

Solar-B EUV Imaging Spectrometer (EIS)




**Time-Dependent Collisional Radiative Model for Iron Line Atomic Data**

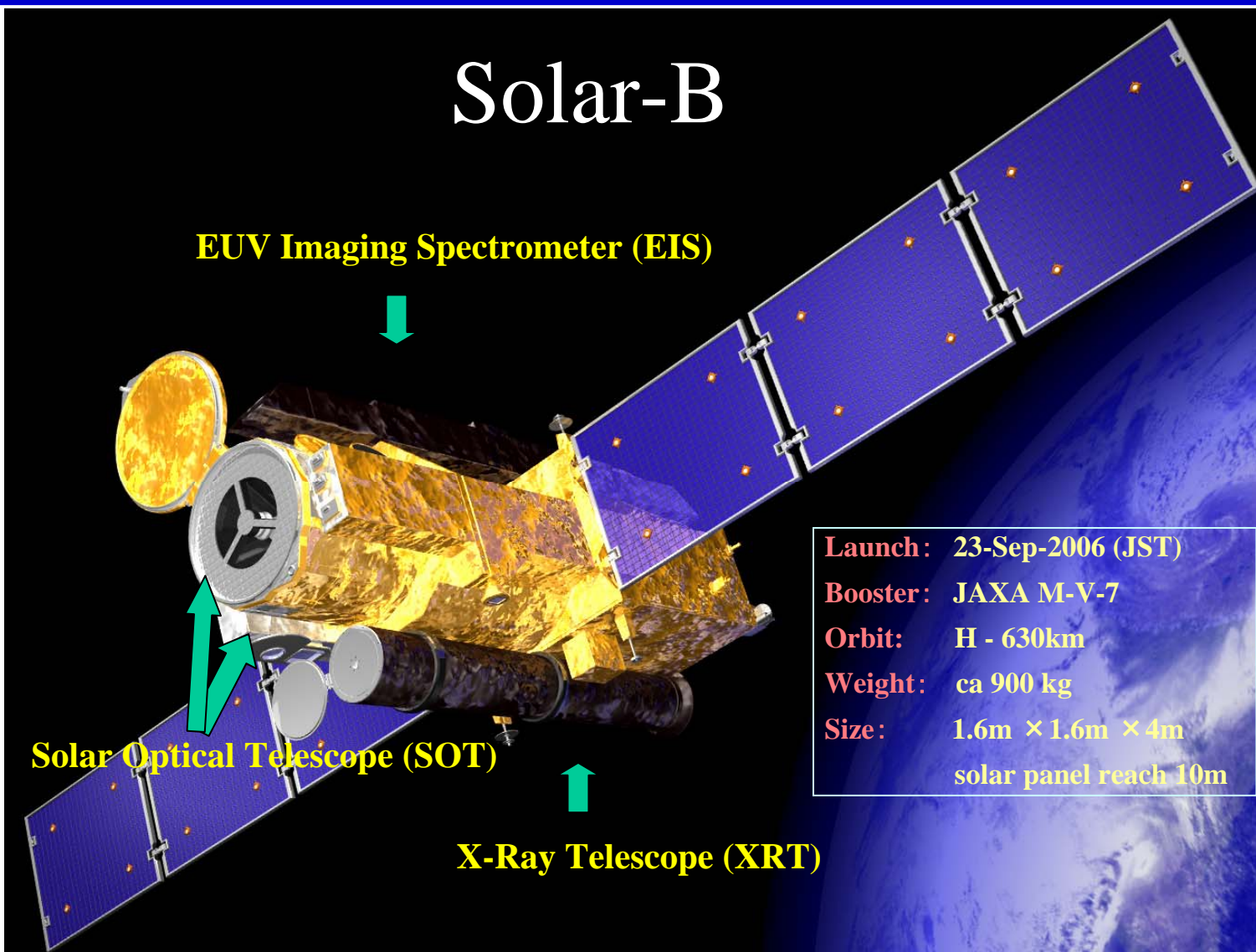


LHD Plasma

## Solar-B (NAOJ) & Large Helical Device (NIFS) Iron M-shell Lines

- Solar-B EIS (NAOJ, JAXA/MSSL/BU/RAL/NRL/UO)
- Atomic Data Evaluation (NIFS)
- Time-dependent Collisional Radiative Model  
Theoretical Calculation (**Yamamoto et al.**)
- Atomic Data Generation   
EBIS/EBIT experiment (**Sakaue et al.**)

## Solar and LHD (Large Helical Device) Plasma Diagnostics in EUV



## Solar and LHD (Large Helical Device) Plasma Diagnostics in EUV



Launch: 23-Sep-2006 6:36am (JST)



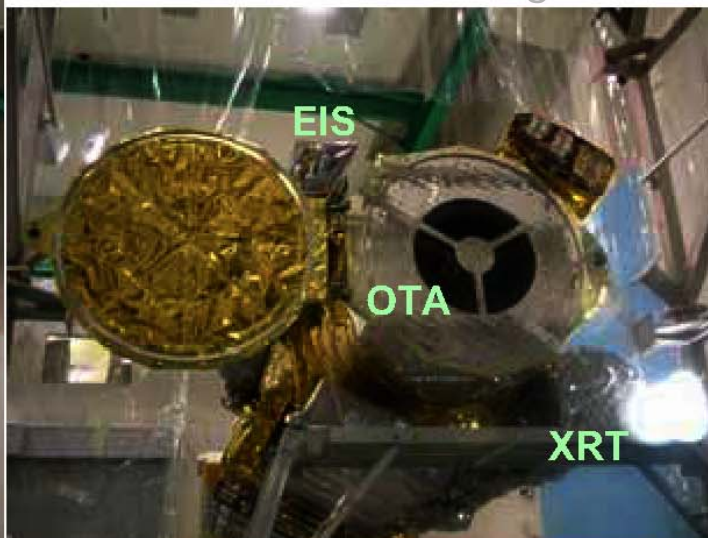
M-V Booster



Uchinoura Space Centre/JAXA

OTA: Optical Telescope Assmby

FPP: Focal Plane Package



XRT: X-ray Telescope

EIS: EUV Imaging Spectrometer



# Uchinoura Space Centre



*Tetsuya Watanabe (NAOJ) et al.*

# Uchinoura Space Centre



*Tetsuya Watanabe (NAOJ) et al.*

## *Hinode* (sunrise; “he-know-day”)

- Epoch: 2006/10/3 18:00:00UTC
- semi-major axis : 7059.706 km
- eccentricity : 0.0000
- inclination : 98.090 deg
- altitude of perigee : 678.452 km
- altitude of apogee : 684.682 km
- period : 98.387 min

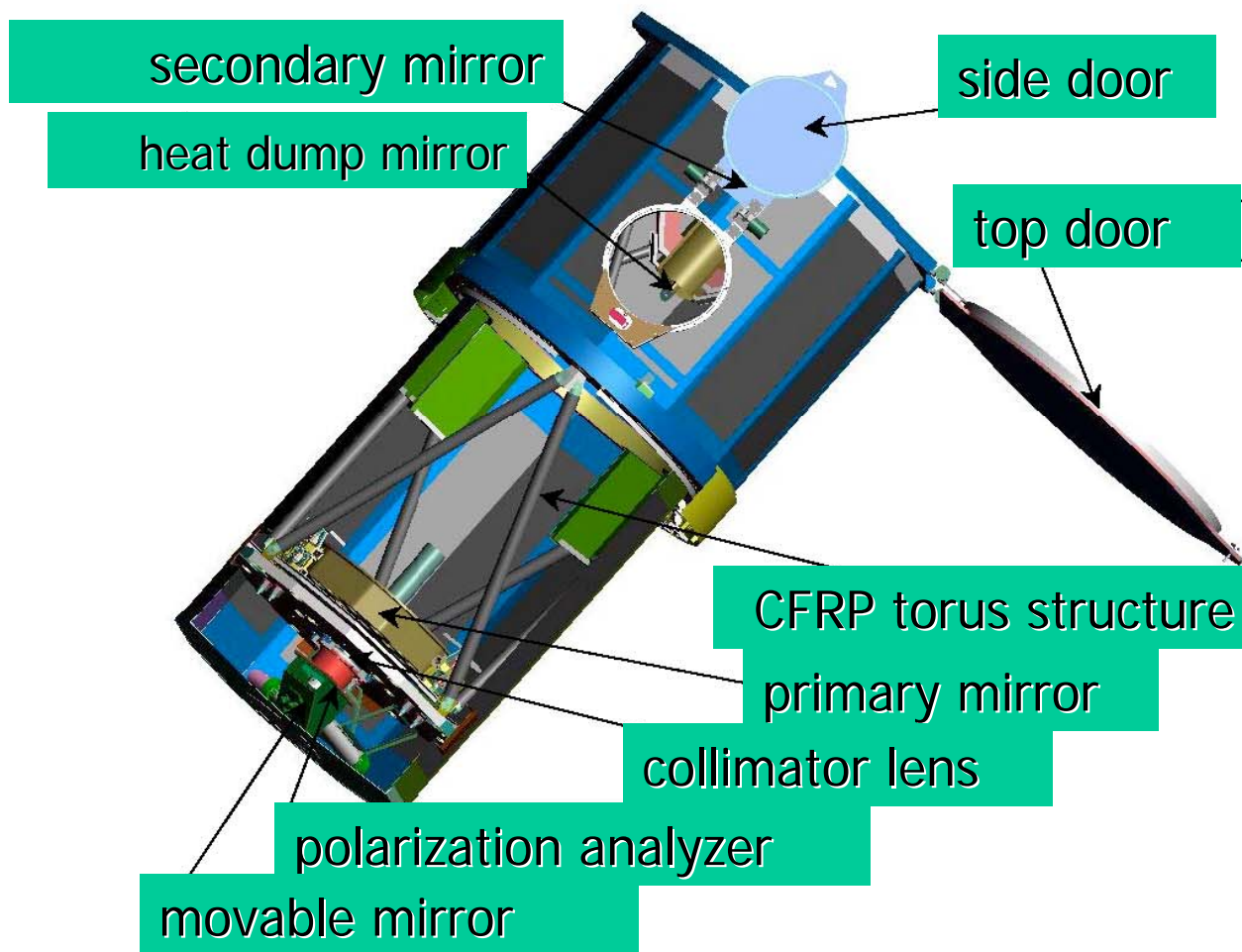


## Opening of Telescope Doors (schedule)

- SOT side door; 14-Oct – **done!**  
top door; 25-Oct
- XRT top door; 27-Oct
- EIS clamshell-front door; 27-Oct  
clamshell-rear door; 28-Oct

## SOT

### Optical Telescope Assembly (OTA)



# SOT

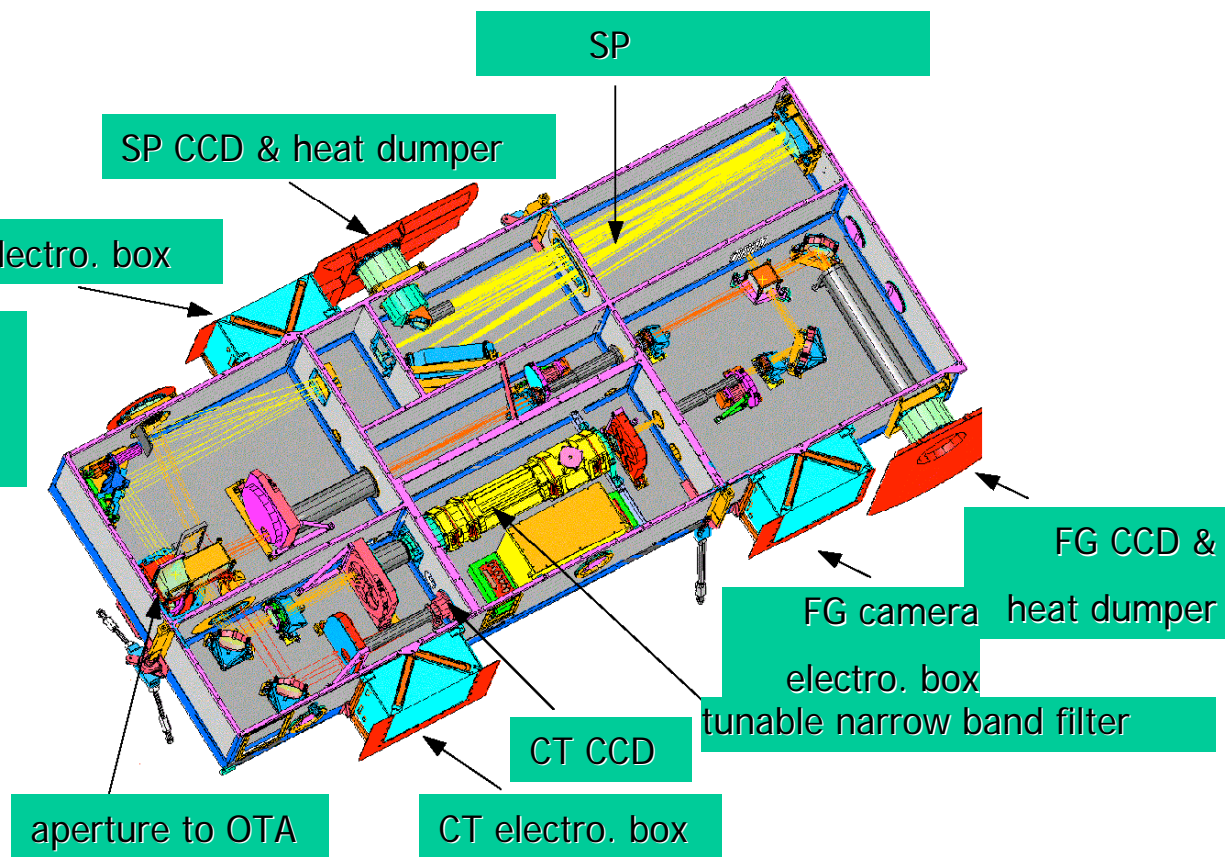
## Focal Plane Package (FPP)

### Filtergraph (FG)

high time-resolution  
2D pictures + 3D  
magnetic fields  
in 12 wavelengths

### Spectropolarimeter (FPP)

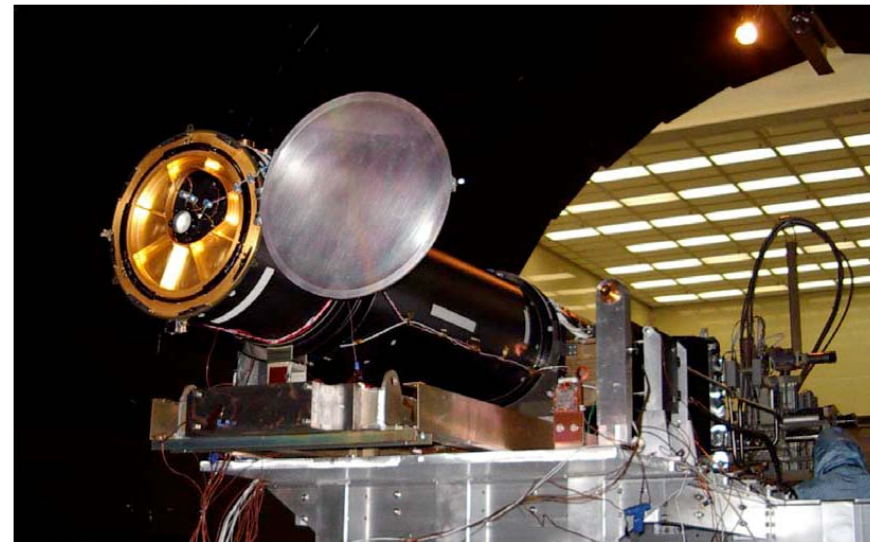
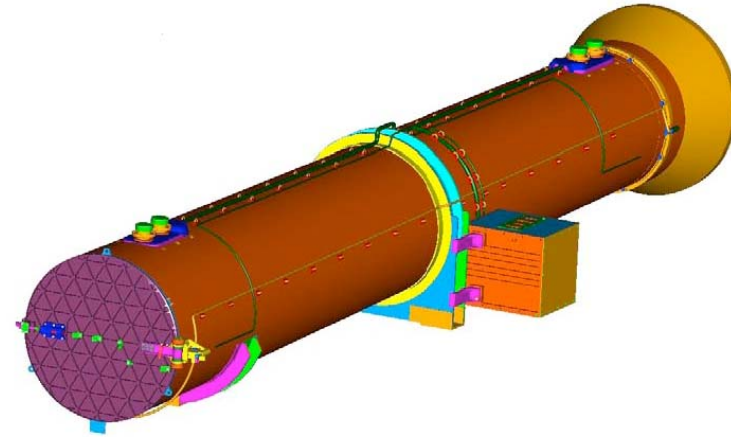
detailed spectro-polarimetry  
of FeI absorption line at  
630nm for 3-D structures of  
photospheric magnetic fields



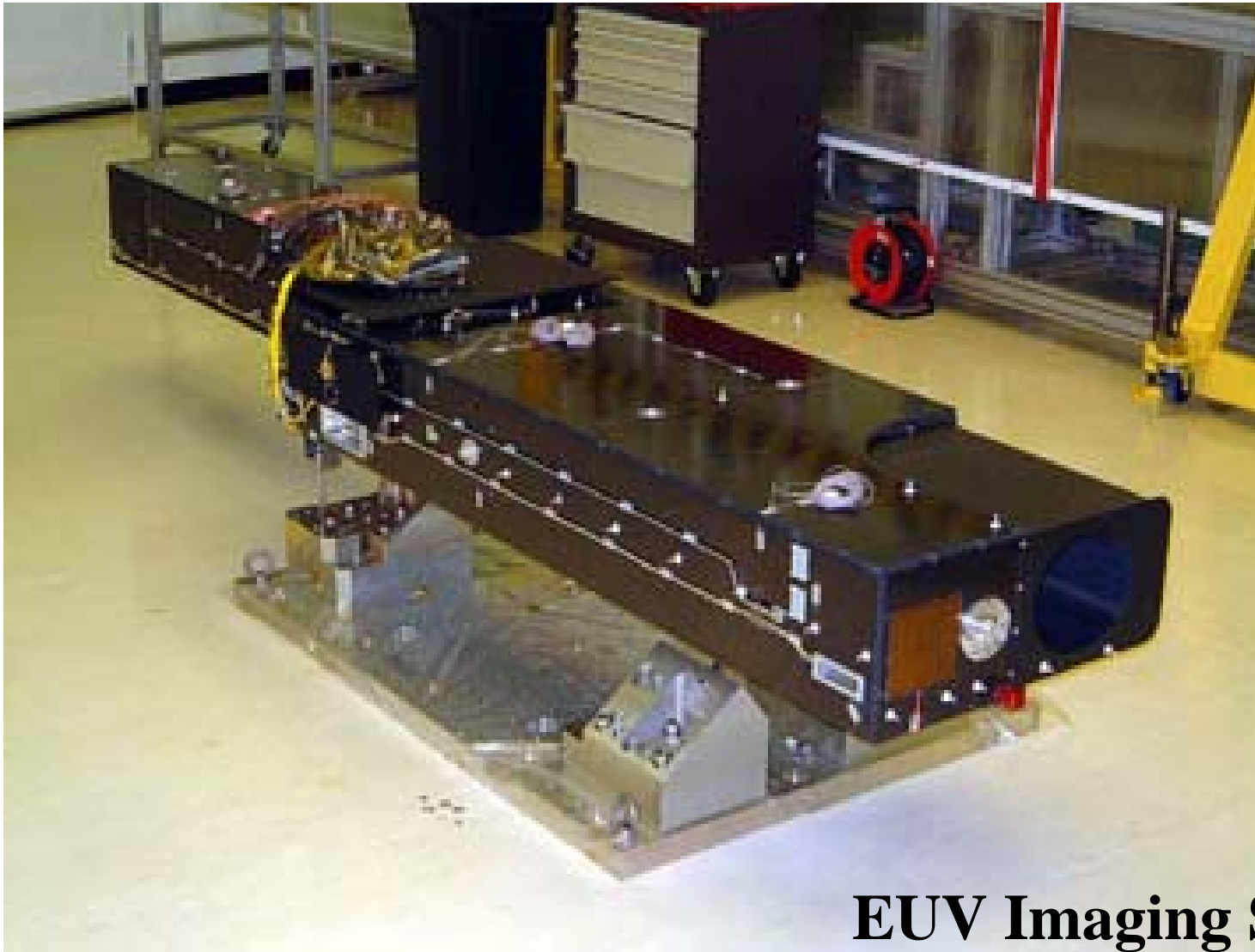
# X-Ray Telescope (XRT)

Takes X-ray images of dynamically changing solar coronal structures

- grazing-incidence telescope + 2k x 2k – pixel CCD to take X-ray images of solar corona
- angular resolution 1" (x 3 better than *Yohkoh*)
- Seeing plasma with temperatures 1 - 10 MK.



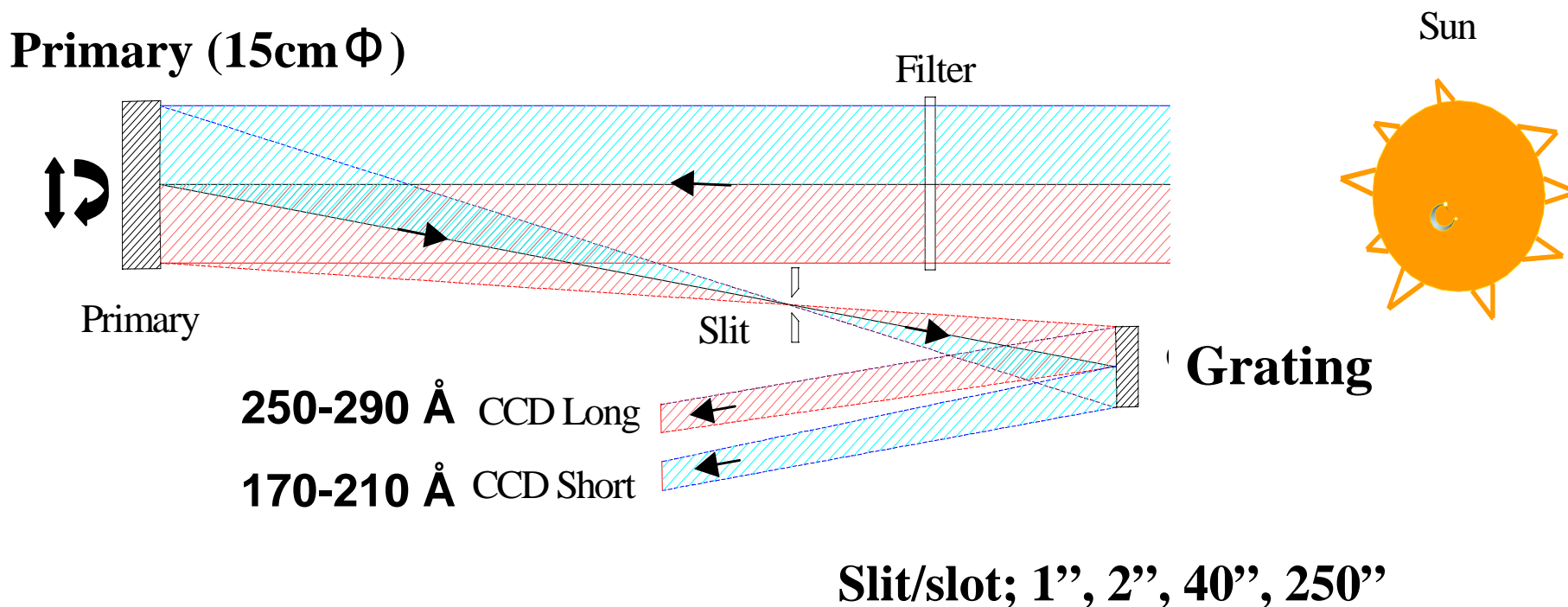
## Solar and LHD (Large Helical Device) Plasma Diagnostics in EUV



**EUV Imaging Spectrometer (EIS)**

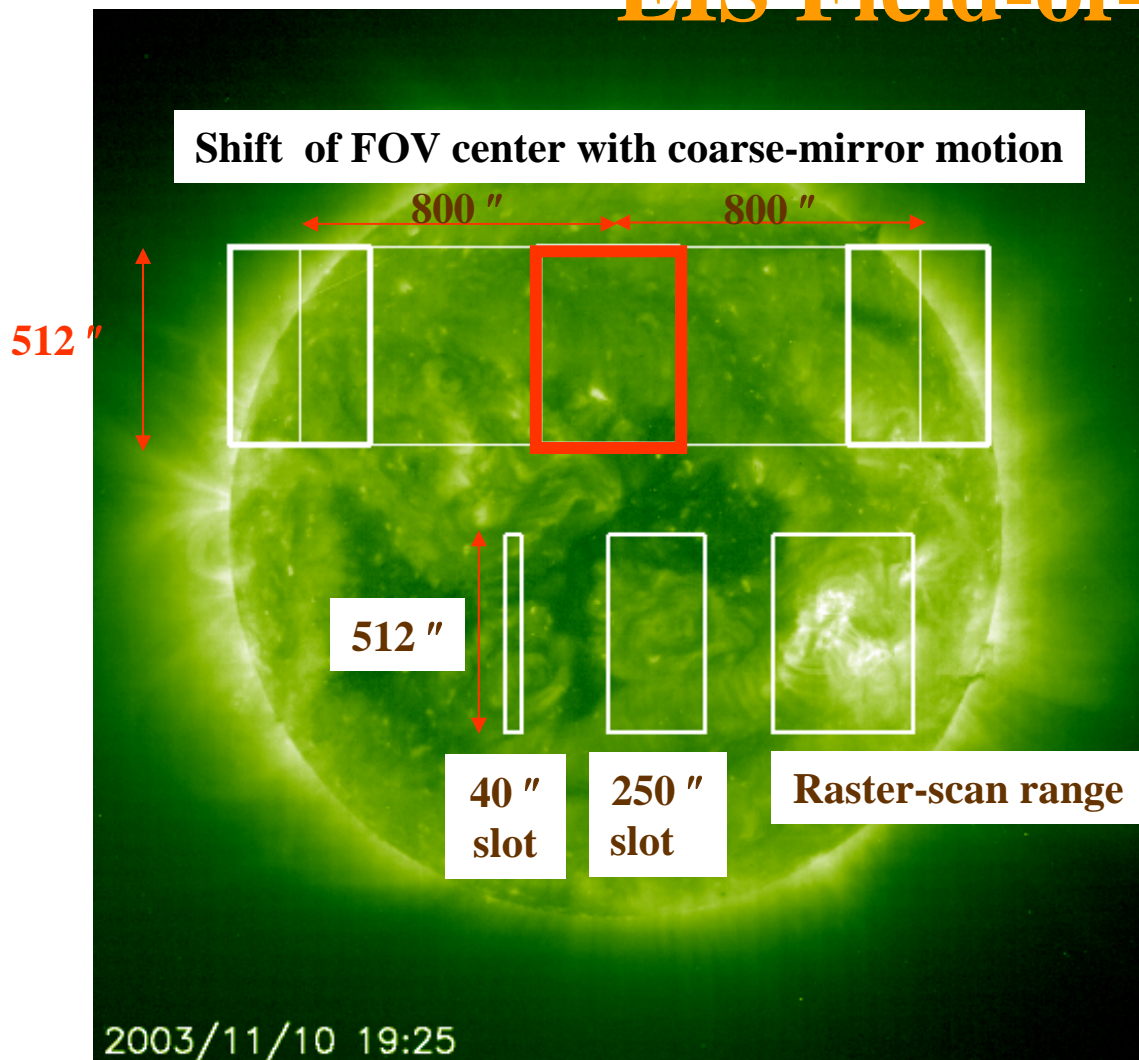
*Tetsuya Watanabe (NAOJ) et al.*

## EIS Optical Path

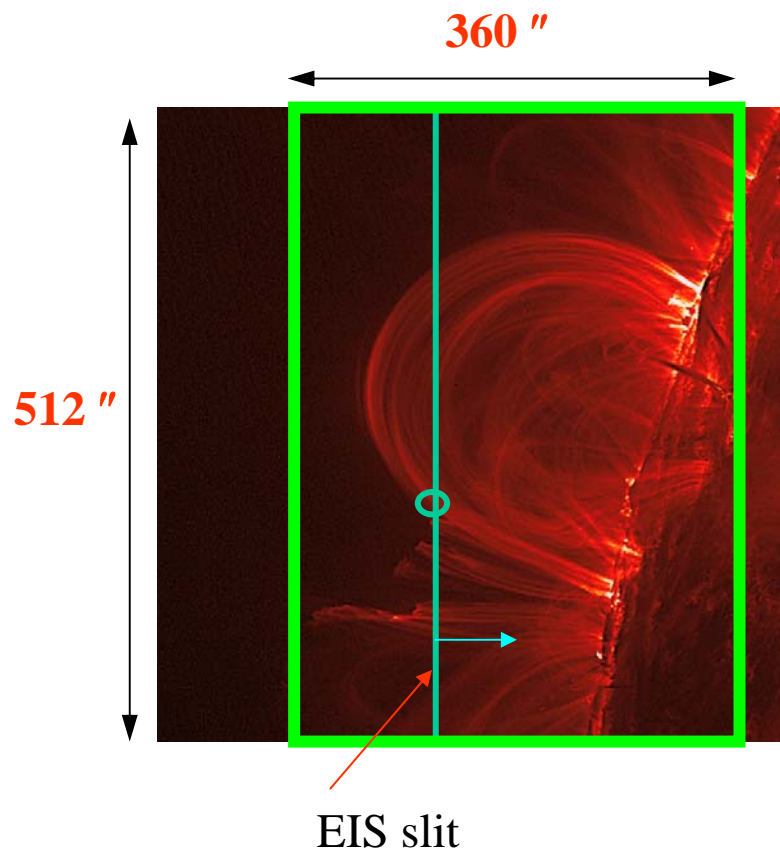


|                            |   |
|----------------------------|---|
| <b>FOV</b>                 | <b>Fine Mirror Scan 360 arcsec</b><br><b>Slit/Slot 1", 2", 40", 250" (4-positions)</b><br><b>Slit length 512 arcsec (1pixel=13.5<math>\mu</math>m=1arcsec)</b>  |
| <b>Min. Exp. Time</b>      | <b>&lt; 1 sec (sit&amp;stare/overlappograph), &lt;1.3sec</b>  |
| <b>Wavelengths</b>         | <b>170 - 210<math>\text{\AA}</math> &amp; 250 - 290<math>\text{\AA}</math></b>  |
| <b>Temperature Range</b>   | <b><math>10^5 - 2 \times 10^7</math> ° K (via HeII ~ FeXXIV)</b>  |
| <b>Density Diagnostics</b> | <b><math>10^8 - 10^{12}</math> cm<sup>-3</sup> (via FeXII)</b>  |
| <b>Velocity Field</b>      | <b><math>\Delta v \sim 20</math> kms<sup>-1</sup>/pix (250 – 290<math>\text{\AA}</math>); 1000ph <math>\rightarrow</math><br/><b>1kms<sup>-1</sup> (line center) , 3kms<sup>-1</sup> (line width)</b></b> |

### EIS Field-of-View (FOV)

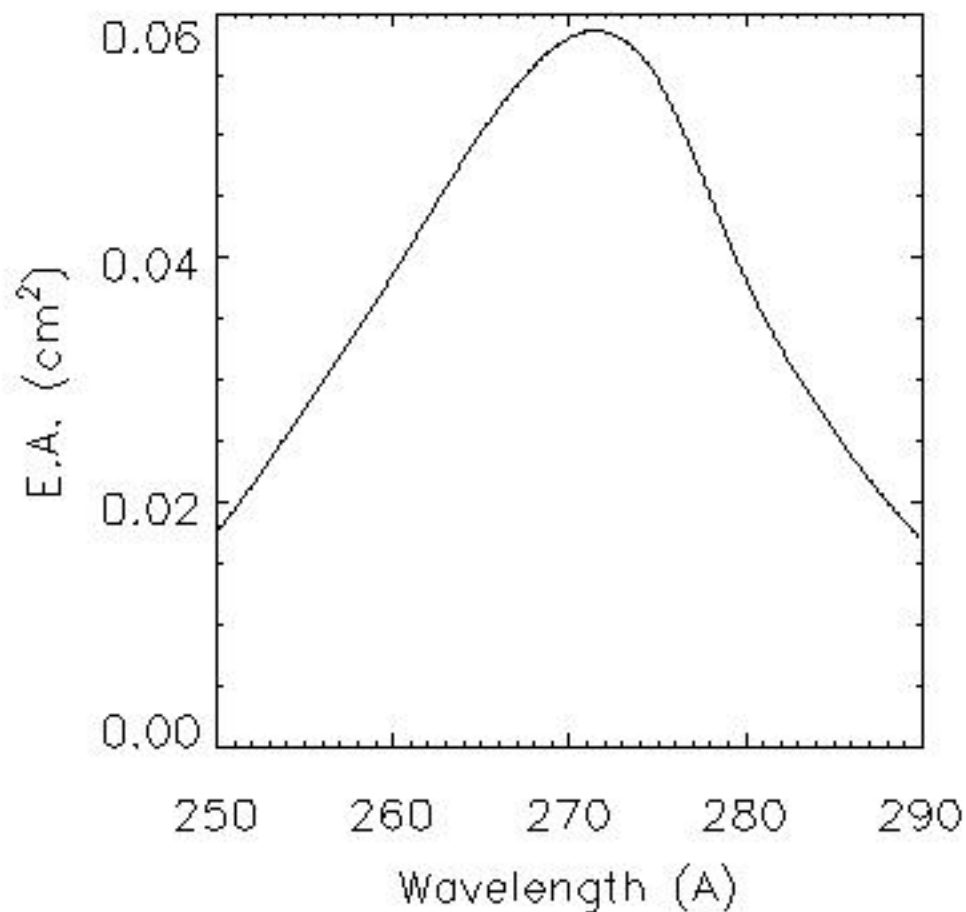
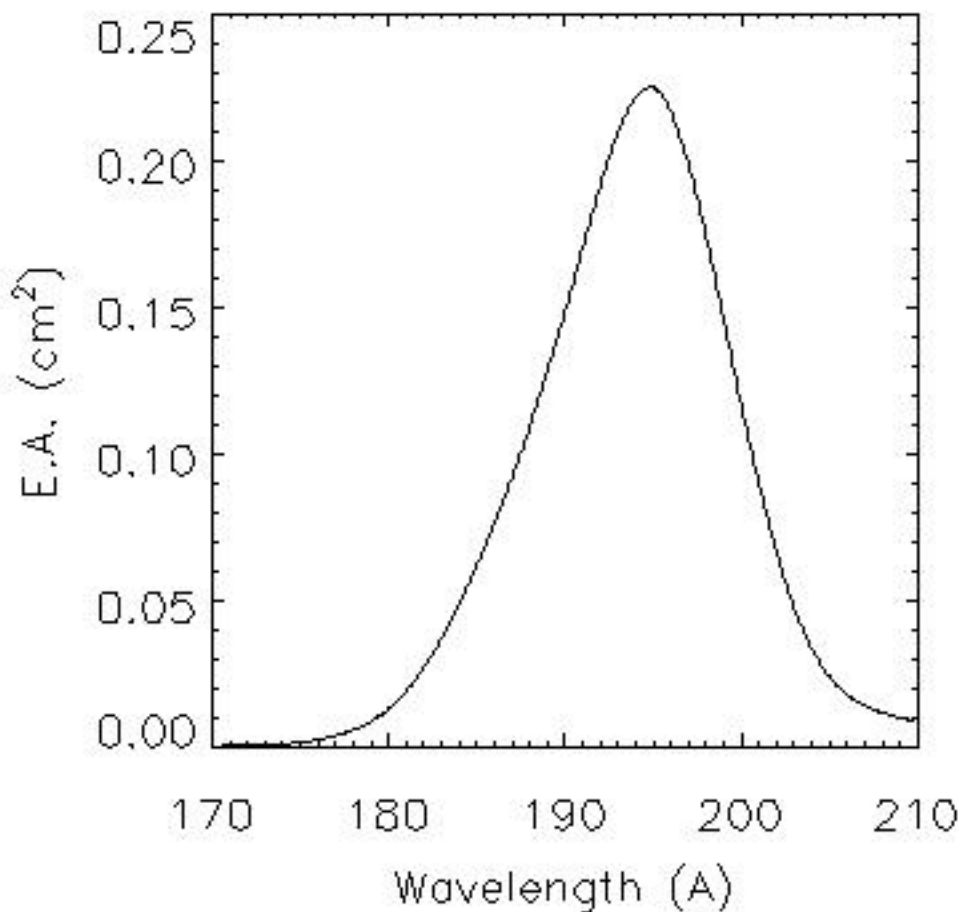


Maximum FOV for raster observation





## EIS Effective Area

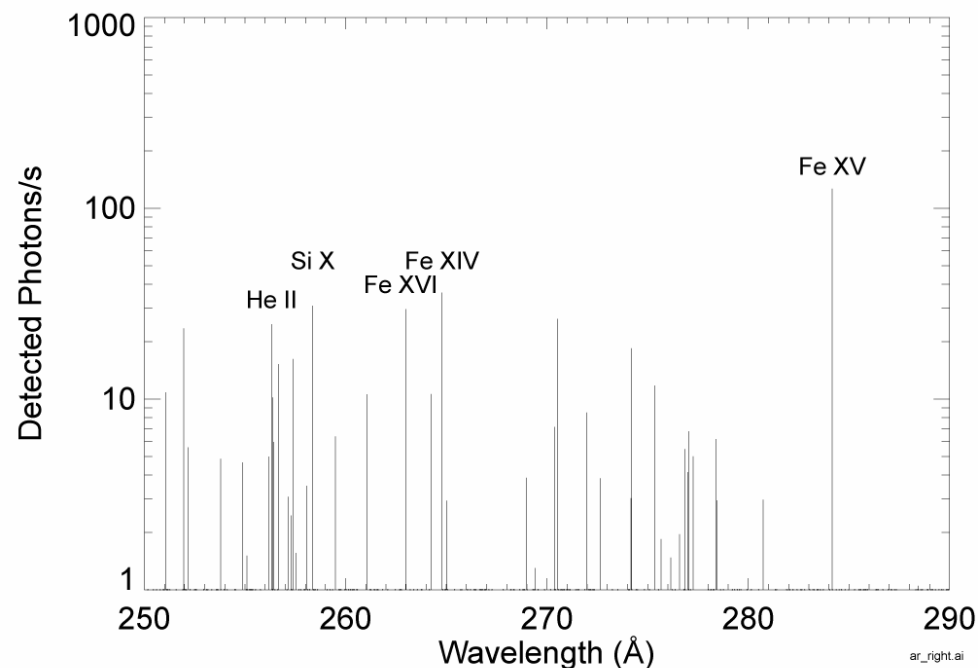
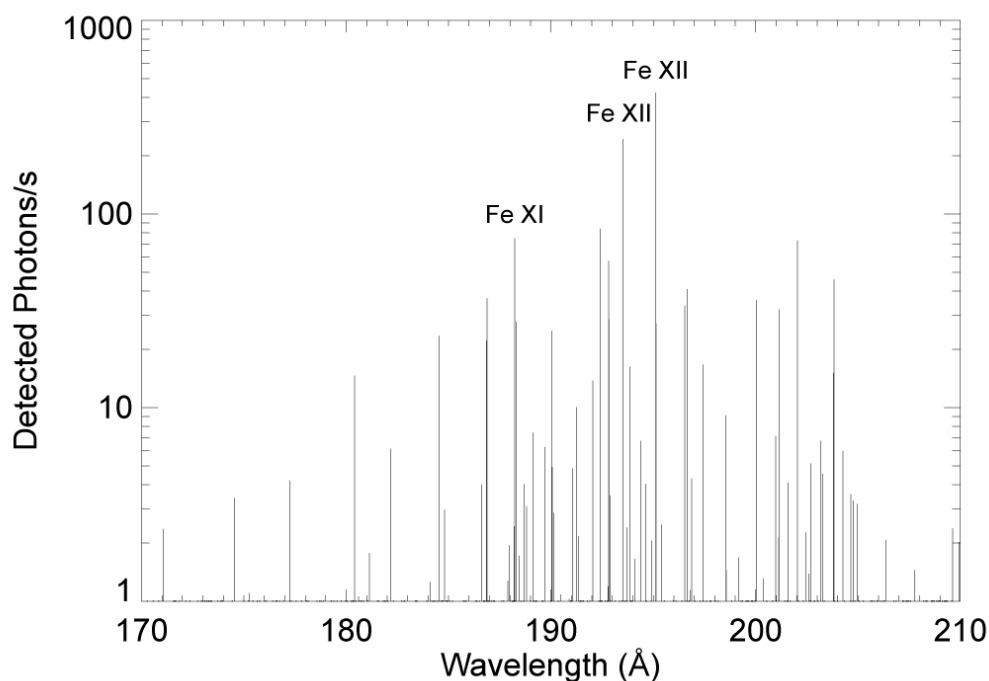


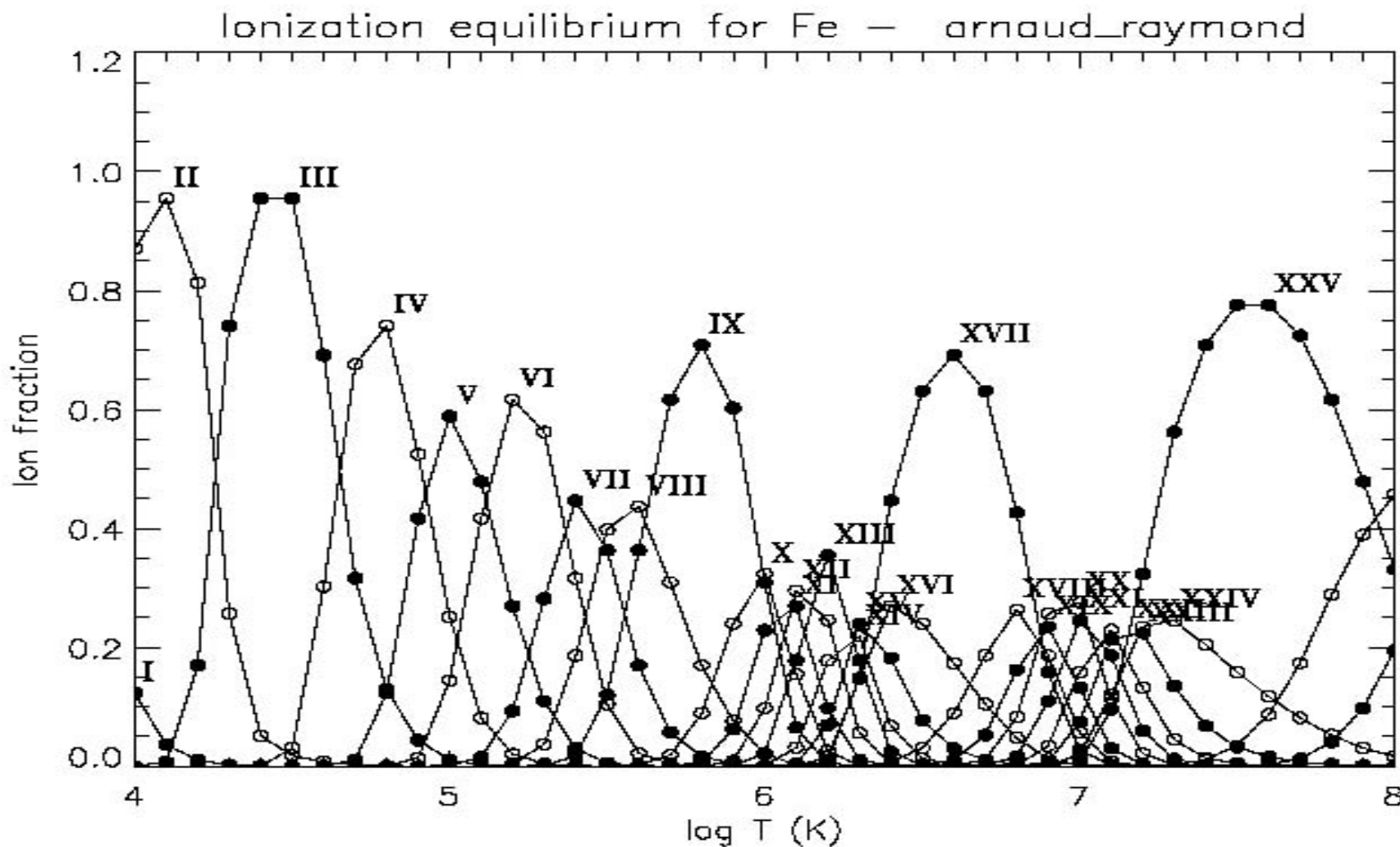
| Ion                   | Wave   | T    | Incident | Detected |
|-----------------------|--------|------|----------|----------|
| Short Wavelength Band |        |      |          |          |
| Fe XI                 | 180.41 | 6.11 | 690.49   | 14.62    |
| Fe X                  | 184.54 | 6.00 | 286.53   | 23.47    |
| Fe XII                | 186.85 | 6.11 | 142.80   | 22.20    |
| Fe XII                | 186.88 | 6.11 | 233.69   | 36.61    |
| Fe XI                 | 188.23 | 6.11 | 359.34   | 74.79    |
| Fe XI                 | 188.30 | 6.11 | 131.76   | 27.77    |
| Fe X                  | 190.04 | 6.00 | 89.48    | 24.95    |
| S XI                  | 191.27 | 6.20 | 31.00    | 10.04    |
| Fe XXIV               | 192.04 | 7.30 | 39.46    | 13.78    |
| Fe XII                | 192.39 | 6.11 | 233.45   | 83.94    |
| Ca XVII               | 192.82 | 6.70 | 154.30   | 57.24    |
| Fe XI                 | 192.83 | 6.11 | 76.80    | 28.51    |
| Fe XII                | 193.52 | 6.11 | 631.78   | 244.11   |
| Ca XIV                | 193.87 | 6.51 | 41.57    | 16.31    |
| Fe XII                | 195.12 | 6.11 | 1052.18  | 424.08   |
| Fe XII                | 195.13 | 6.11 | 67.64    | 27.26    |
| Fe XIII               | 196.54 | 6.20 | 86.19    | 33.58    |
| Fe XII                | 196.65 | 6.11 | 105.45   | 40.83    |
| Fe XIII               | 197.43 | 6.20 | 45.80    | 16.67    |
| Fe XIII               | 200.02 | 6.20 | 155.95   | 36.00    |
| Fe XIII               | 201.13 | 6.20 | 192.59   | 32.15    |
| Fe XIII               | 202.04 | 6.20 | 591.85   | 72.96    |
| Fe XIII               | 203.80 | 6.20 | 208.79   | 15.09    |

| Ion                  | Wave   | T    | Incident | Detected |
|----------------------|--------|------|----------|----------|
| Fe XIII              | 203.83 | 6.20 | 638.82   | 45.80    |
| Long Wavelength Band |        |      |          |          |
| Fe XVI               | 251.07 | 6.40 | 188.12   | 10.84    |
| Fe XIII              | 251.96 | 6.20 | 387.52   | 23.48    |
| He II                | 256.32 | 4.70 | 328.81   | 24.69    |
| He II                | 256.32 | 4.70 | 164.40   | 12.34    |
| Si X                 | 256.38 | 6.11 | 135.28   | 10.18    |
| S XIII               | 256.68 | 6.40 | 199.87   | 15.23    |
| Fe XIV               | 257.38 | 6.30 | 207.85   | 16.23    |
| Si X                 | 258.37 | 6.11 | 382.83   | 30.83    |
| Si X                 | 261.06 | 6.11 | 123.07   | 10.58    |
| Fe XVI               | 262.98 | 6.40 | 331.16   | 29.55    |
| S X                  | 264.23 | 6.11 | 116.73   | 10.62    |
| Fe XIV               | 264.78 | 6.30 | 394.57   | 36.15    |
| Fe XIV               | 270.51 | 6.30 | 291.23   | 26.31    |
| Fe XIV               | 274.20 | 6.30 | 241.91   | 18.46    |
| Si VII               | 275.35 | 5.80 | 166.99   | 11.76    |
| Fe XV                | 284.16 | 6.30 | 4063.11  | 126.55   |

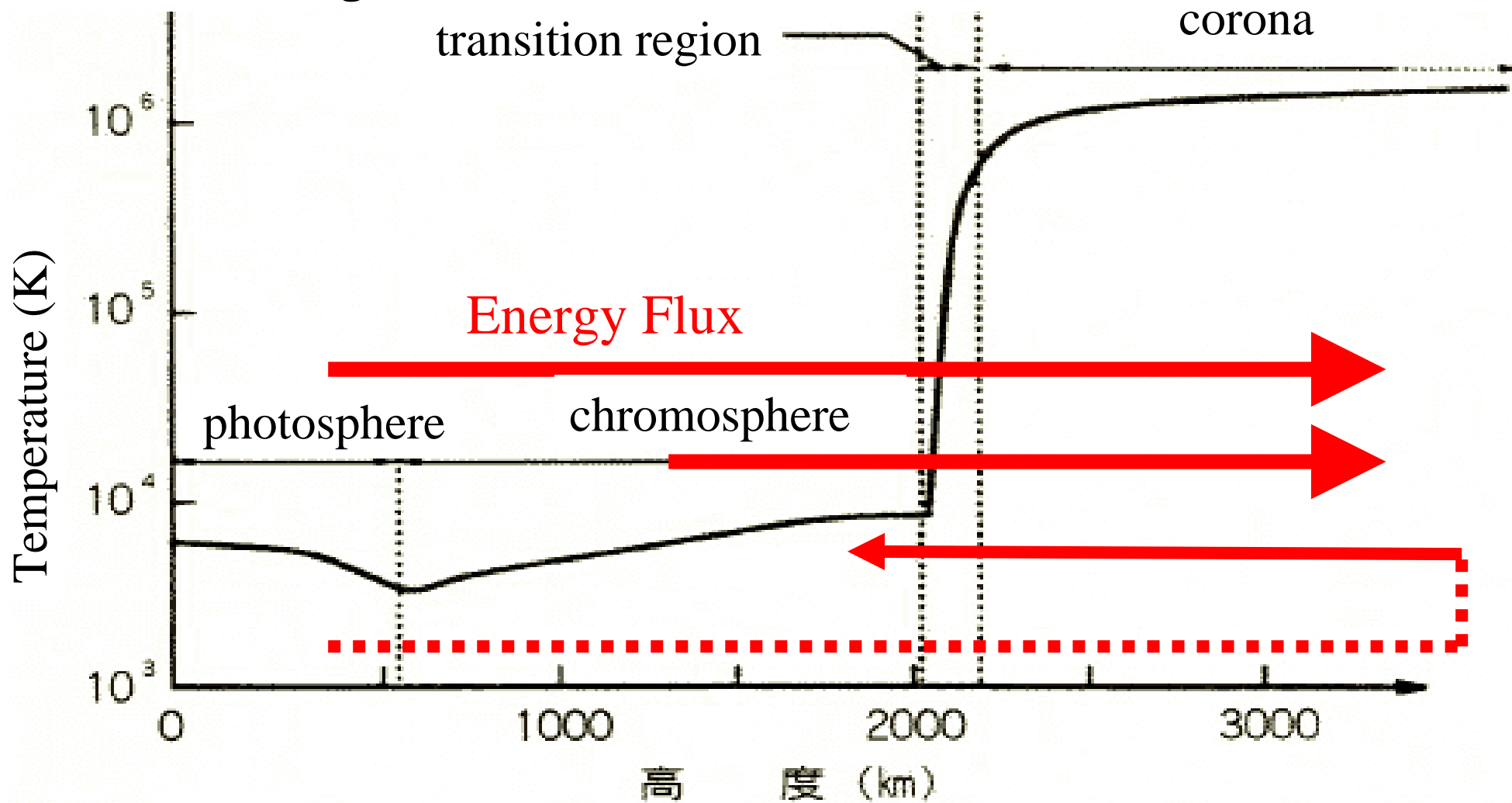
**Active Region**

## Active Region

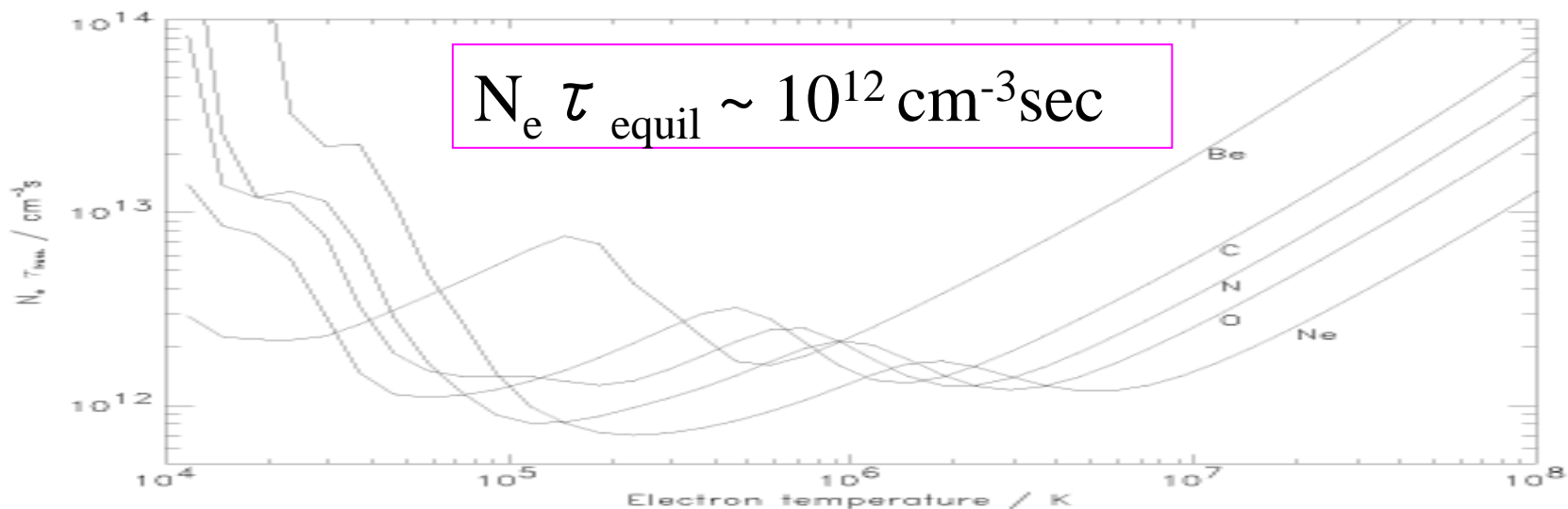




## Coronal Heating Mechanism



## Ionization Equilibrium; Relaxation Time Scales



*Brooks et al. (1999)*

|                    | $N_e(\text{cm}^{-3})$                            | $T_e(\text{K})$                           | $\tau_{transient}$              |
|--------------------|--|---|---------------------------------|
| upper chromosphere | $3.7 \times 10^{10}$                             | $2 \times 10^4$                           | $\sim 5 \rightarrow 6$ minutes  |
| transition region  | $1.3 \times 10^{10} \rightarrow 1.3 \times 10^9$ | $5 \times 10^4 \rightarrow 5 \times 10^5$ | $\sim 3 \rightarrow 20$ minutes |
| corona             | $5.4 \times 10^8$                                | $1 \times 10^6$                           | $\sim 1$ hour                   |

## Iron M-shell Line Atomic Data Evaluation

### Fe X, Fe XI, Fe XIII

- Survey existing data
- Method of Calculation
- Pick up Recommended data
- Analytical fitting (only) for Fe XIII

## FeXIII

[Fawcett & Mason \(1989\)](#)

SuperStructure, 48 levels, Distorted Wave

[Gupta & Tayal \(1998\)](#)

26 levels, Semirelativistic R-matrix (Breit-Pauli approximation), partial waves with  $J \leq 22.5$ ,  $E < 60 \text{ Ryd}$

[Tayal \(2000\)](#)

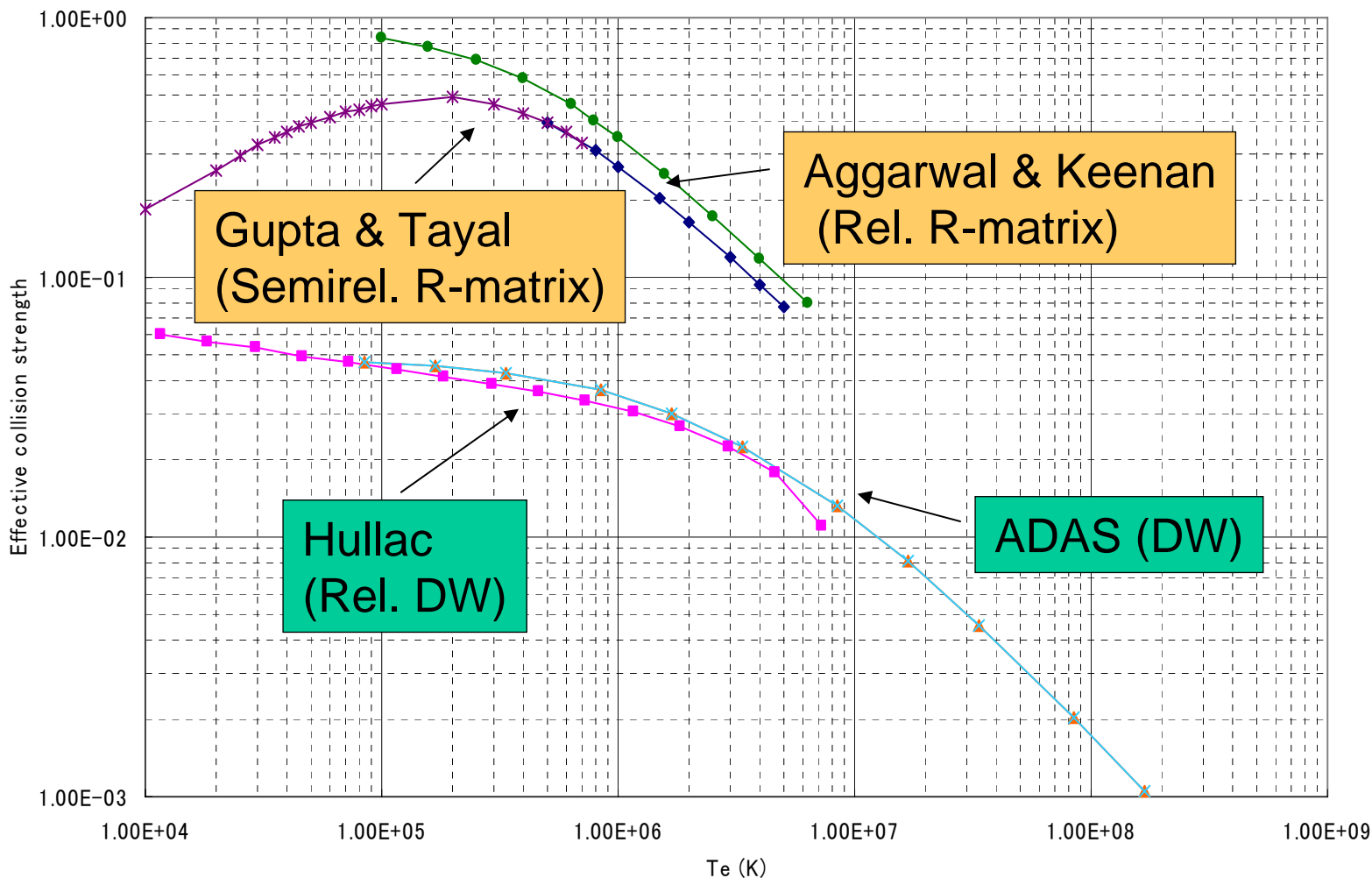
26 levels, Breit-Pauli R-matrix,  $E < 90 \text{ Ryd}$ , partial waves with  $J \leq 22.5$ ,  $0.005 \text{ Ryd}$  mesh

[Aggarwal & Keenan \(2005\)](#)

GRASP, 97 levels, **Dirac Atomic R-matrix**,  $E < 120 \text{ Ryd}$ , partial waves with  $J \leq 39.5$ ;  $0.001\text{-}0.002 \text{ Ryd}$  mesh



Fe XIII 3s2 3p2 3P0 - 3P1



Effective collision strengths :  
Fe XIII  
 $3s^2 3p^2 \ ^3P_0 - \ ^3P_1$

- Hullac3
- ▲ adas-hm
- ✕ adas-al97
- ◆ Gupta, G.P., Tayal, S.S. (1998)
- ✱ Tayal, S.S. (2000)
- Aggarwal, K.M., Keenan, F.P. (2005)

## RESULTS

## Electron-Ion Collisions

Fe X

➤ **Aggarwal, K. M., & Keenan, F. P., A&A, 439, 1215 (2005)**

fully relativistic approach based on GRASP code for the generation of wavefunctions, and the Dirac Atomic *R*-matrix Code (DARC) for the computations collision and effective collision strengths. Calculations are in the *jj* coupling scheme, and Breit and QED corrections have been included.

### Advantages of this work:

- significantly improved the accuracy of energy levels, radiative rates and collision strengths, by including extensive CI and performing the calculations in the *jj* coupling.
- improving the accuracy of  $\Omega$  values by extending the range of partial waves and by achieving convergence in values of  $\Omega$  at all energies and the energy range considered
- improving the  $\Gamma$  values by resolving resonances in a finer energy mesh and by including additional resonances
- extending the range of levels and including many of the desired levels among which the transitions have already been observed

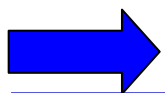
**The results presented in paper Aggarwal & Keenan have obvious advantages in comparison with all earlier results.**

In comparison with the work Bhatia & Doschek, these calculations have significantly improved the accuracy of energy levels, radiative rates and collision strengths, by including extensive CI and performing the calculations in the *jj* coupling.

Fe X

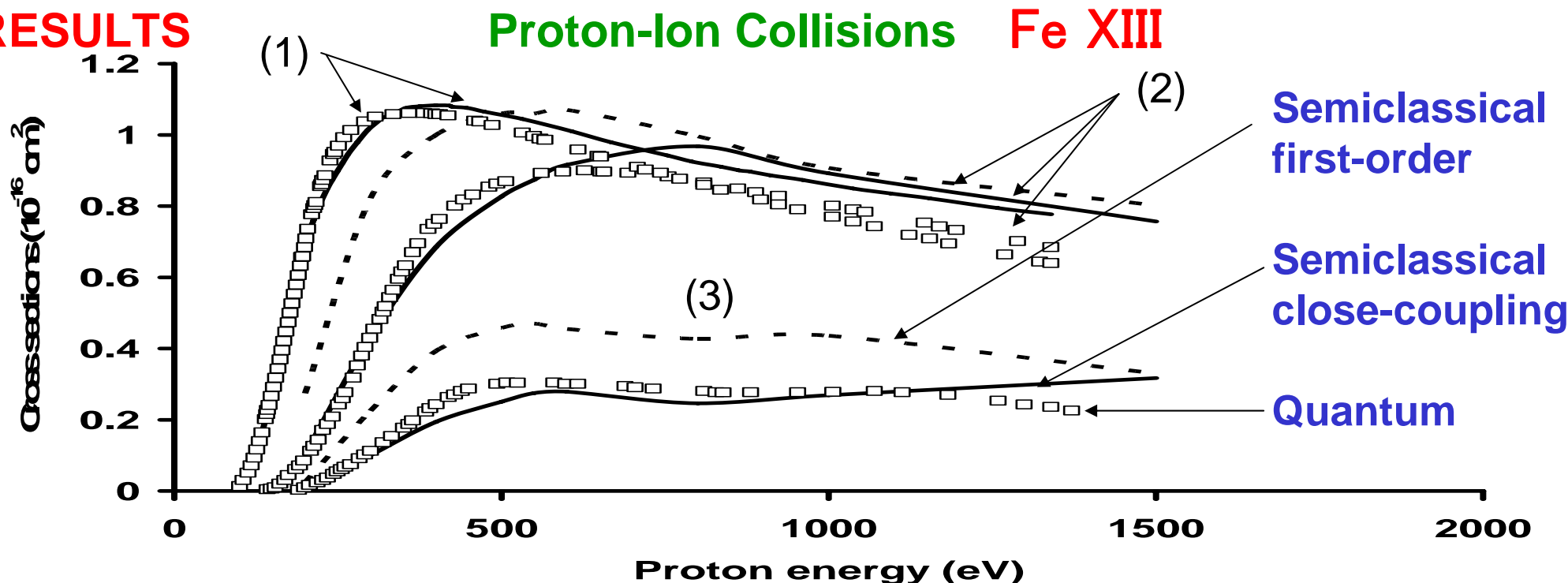
In comparison to the work Tayal an overall improvement has been made by: (i) including additional CI in the generation of wavefunctions, and thus improving the accuracy of energy levels; (ii) extending the range of levels from 54 to 90, and hence including many of the desired levels among which the transitions have already been observed; (iii) improving the accuracy of  $\Omega$  values, by extending the range of partial waves (from 20 to 39) and the energy range (from 90 Ryd to 210 Ryd); (iv) improving the  $\Gamma$  values by resolving resonances in a finer energy mesh and by including additional resonances; (v) performing the calculations in the *jj* coupling instead of the semi-relativistic approach in the *LSJ* coupling scheme.

Similarly, this work is an improvement over the work of Pelan & Berrington mainly by extending the range of levels (transitions) from 31 (465) to 90 (4005), and by achieving convergence in values of  $\Omega$  at all energies.



**We recommend to use for Fe X data of Aggarwal & Keenan.**

### RESULTS



Proton excitation cross sections for transitions in **Si-like Fe XIII**:  $\square$  - quantum results [Faucher 1977], solid line - semi-classical results [Landman 1975], dotted line - semi-classical results [Masnou-Seeuws & McCarroll 1972]; (1) - transition  $^3P_0$ - $^3P_1$ , (2) - transition  $^3P_1$ - $^3P_2$ , (3) - transition  $^3P_0$ - $^3P_2$ .

## RESULTS

## Proton-Ion Collisions

### General conclusion:

In **low density** plasma  $N_e \leq 10^{16} \text{ cm}^{-3}$  proton collisions are Important for ions: **Fe X, XI, XIII, XIV, XVII, XVIII, XIX, XX, XXI, XXII, XXIII.**

In **high density** plasma  $N_e > 10^{16} \text{ cm}^{-3}$  proton collisions are Important for ions: **Fe XV, XVII, XXII.**

$$N_p \sim N_e < A_i / C_i^e$$

For Fe XII proton collisions are not important.

For all important transitions we have evaluated available numerical data and recommended data were fitted to analytical formula.

## Collisional-radiative model -Atomic Processes &Energy Levels

### Atomic Processes (*rate*):

Excitation/de-excitation ( $C^e N_e$ ) by e<sup>-</sup>-impact,

**Excitation/de-excitation ( $C^p N_e$ ) by p-impact,**

Ionization ( $S N_e$ ) /three-body recombination ( $\beta^t N_e^2$ ),

Radiative transition ( $A^r$ ), Radiative recombination ( $\beta^r N_e$ )

### Energy Levels (*configuration*): $2 \leq n \leq 5$

Bare, H-like( $nl$ ), He-like( $1s nl$ ), Li-like( $1s^2 nl$ ), Be-like( $2l' nl$ ), B-like( $2s^2 nl$ ,  $2s 2p nl$ ,  $2p^2 nl$ ), C-like( $2s^2 2p nl$ ,  $2s 2p^2 nl$ ,  $2p^2 nl$ ), N-like( $2s^2 2p^2 nl$ ,  $2s 2p^3 nl$ ,  $2p^4 nl$ ), O-like( $2s^2 2p^3 nl$ ,  $2s 2p^4 nl$ ,  $2p^5 nl$ ), F-like( $2s^2 2p^4 nl$ ,  $2s 2p^5 nl$ ,  $2p^6 nl$ ), Ne-like ( $2s^2 2p^5 nl$ ,  $2s 2p^6 nl$ ), Na-like( $2s^2 2p^6 nl$ ), Mg-like( $3l' nl$ ), Al-like( $3s^2 nl$ ,  $3s 3p nl$ ,  $3s 3d nl$ ,  $3p^2 nl$ ,  $3p 3d nl$ ), Si-like( $3s^2 3l' nl$ ), P-like( $3s^2 3p 3l' nl$ ), S-like( $3p^2 3l' nl$ ), Cl-like( $3p^3 3l' nl$ ), Ar( $3p^5 nl$ ), K-like( $3p^6 nl$ ,  $3p^5 3d nl$ ), Ca-like( $3p^6 3d nl$ )

## Collisional-radiative model (Yamamoto et al.)

### Time-dependent Rate Equation:

$$\frac{dN_i(t, T_e, N_e)}{dt} = -N_i(t, T_e, N_e) \sum_j W_{ij}(T_e(t), N_e(t)) + \sum_j W_{ji}(T_e(t), N_e(t)) N_j(t, T_e, N_e)$$

### Quasi-steady State Solution:

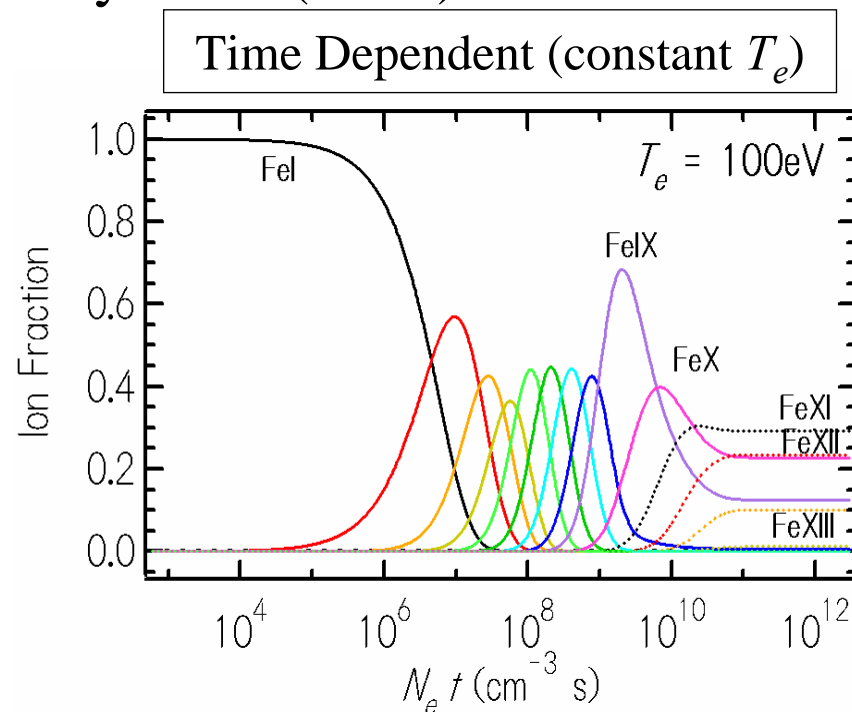
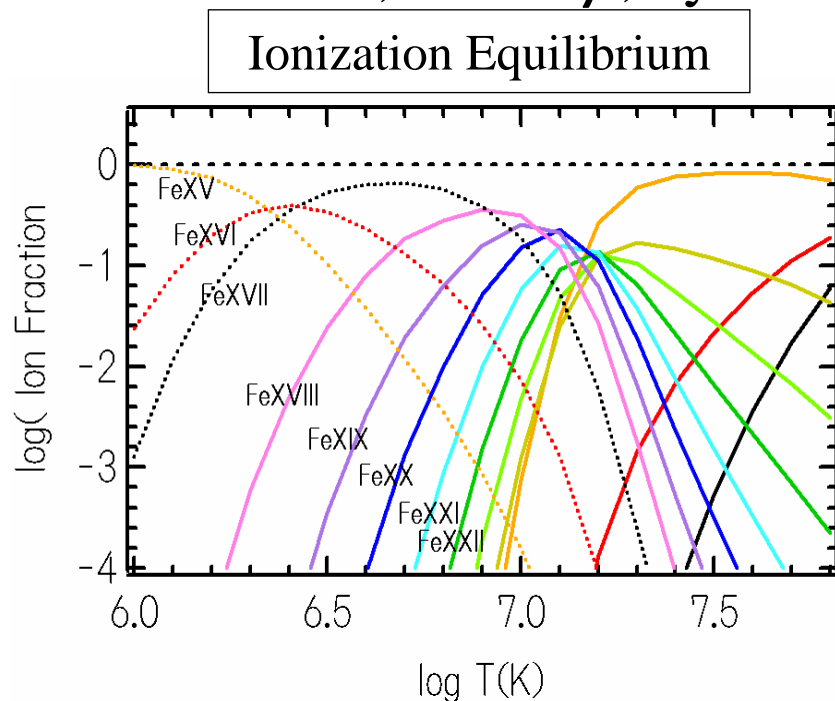
$$N_i(t, T_e, N_e) = \sum_k r_i^{(k)}(T_e, N_e) N_e N_k(t, T_e, N_e)$$

### Time-independent Rate Equation:

$$\frac{dr_i^{(k)}(T_e, N_e)}{dt} = -r_i^{(k)}(T_e, N_e) \sum_j W_{ij}(T_e, N_e) + \sum_j W_{ji}(T_e, N_e) r_j^{(k)}(T_e, N_e)$$

## Ion Fraction $N_k$ :

$N_k$  is calculated to use total ionization and recombination rate coefficients,  $S$  and  $\beta$ , by Arnaud & Raymond (1992).

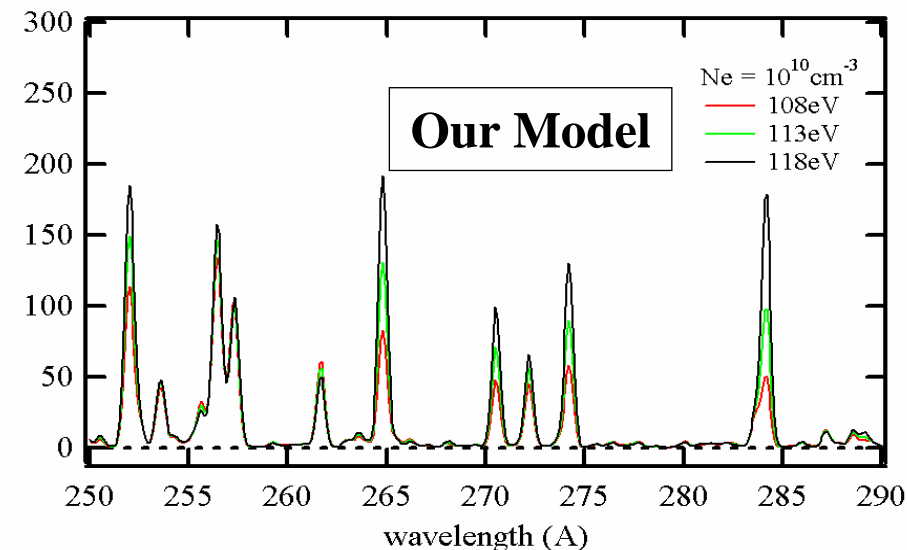
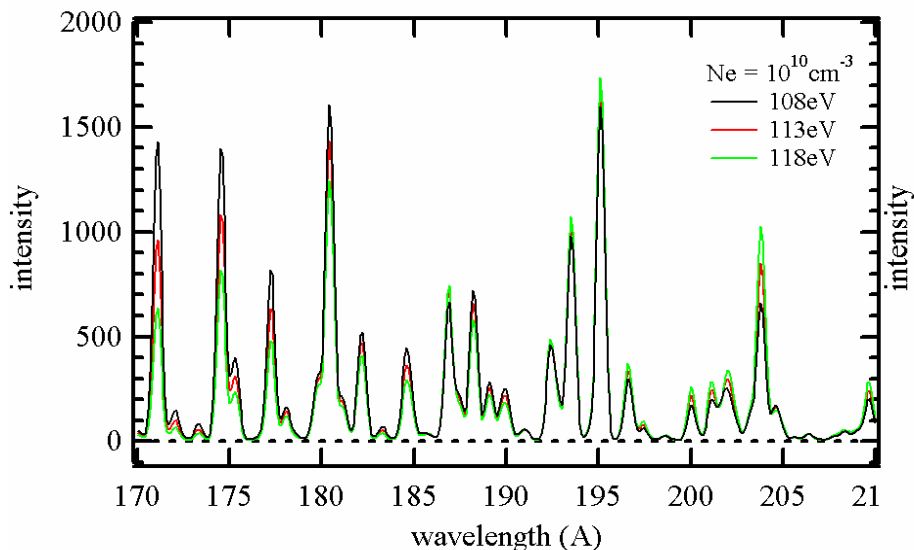
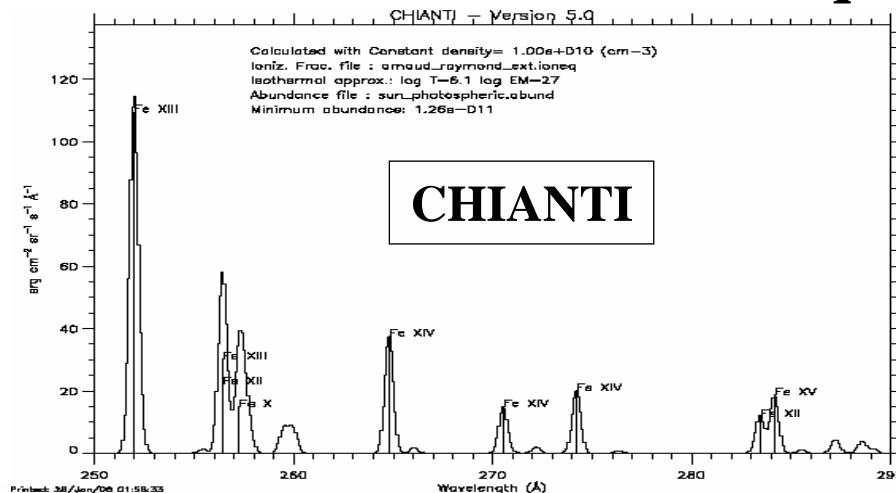
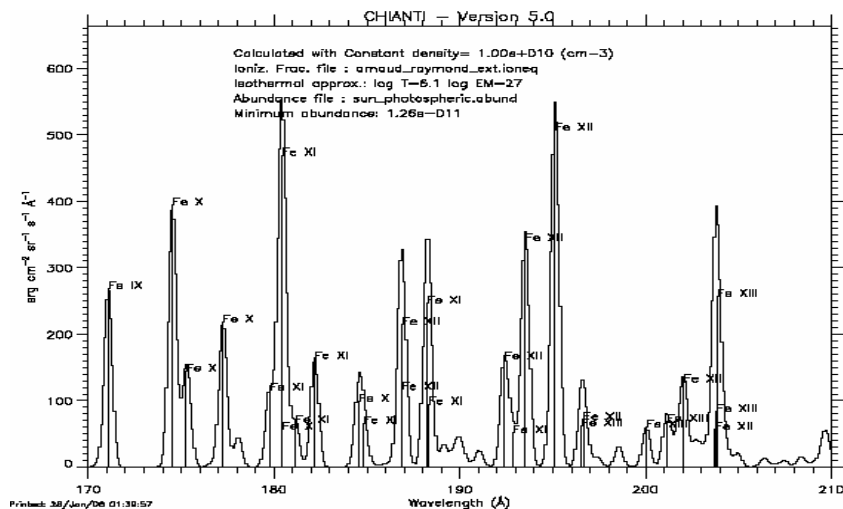


## Line Intensity $I(\lambda)$ : $$I(\lambda) = \sum_i N_i A_{ij}^r \Delta E_{ij} P_i(\lambda)$$

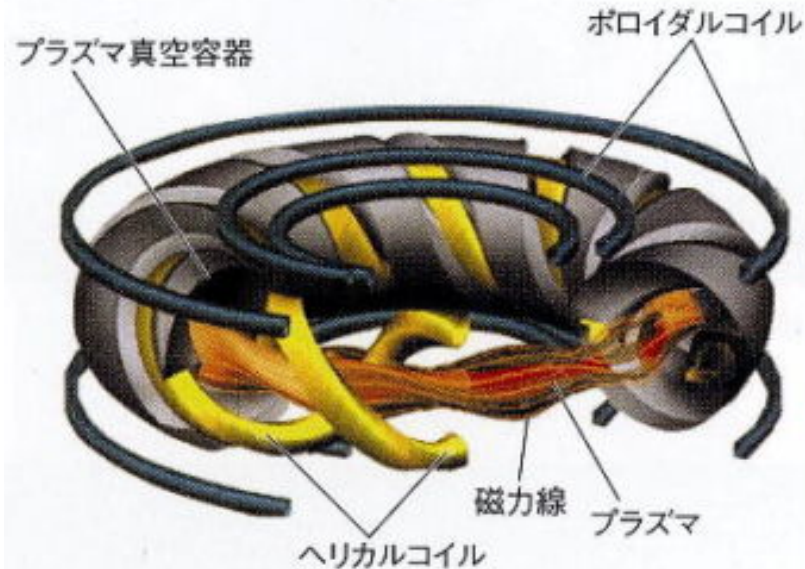
Tetsuya Watanabe (NAOJ) et al.



equilibrium



## Solar and LHD (Large Helical Device) Plasma Diagnostics in EUV

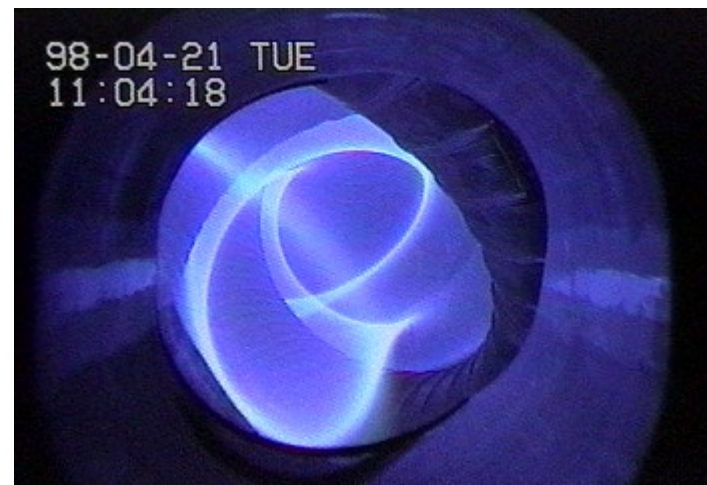


# LHD experiment

Te, ne, V

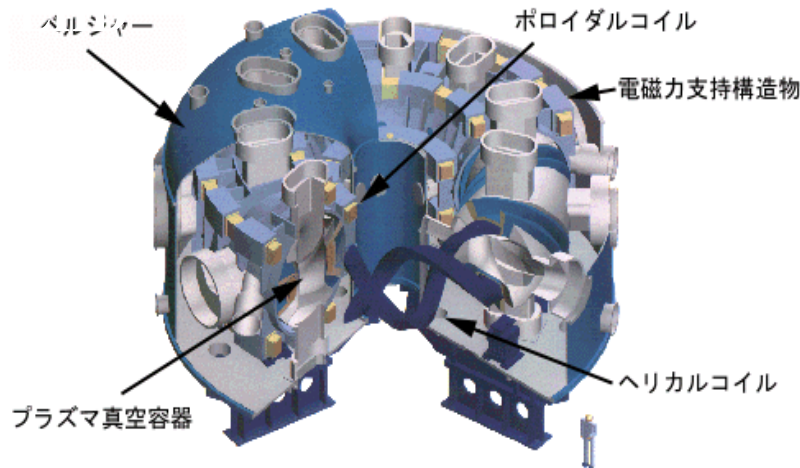
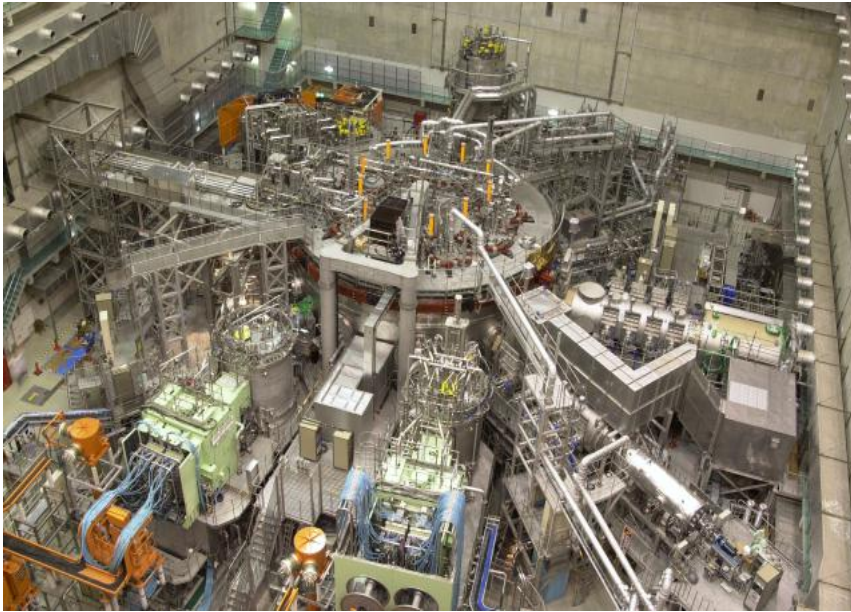


# Diagnostics



## Solar and LHD (Large Helical Device)

### Plasma Diagnostics in EUV



**Plasma Source** : Hydrogen  
with *Fe-pellet* injection

### **Fe-TESPEL** :

*Polystyrene-shell Fe pellet*

Pellet Radius: 780-820 $\mu$ m

Mass of Fe in the shell: 43-66 $\mu$ g

Mass of shell: 250-300 $\mu$ g

Injection Velocity: 300-400m/s

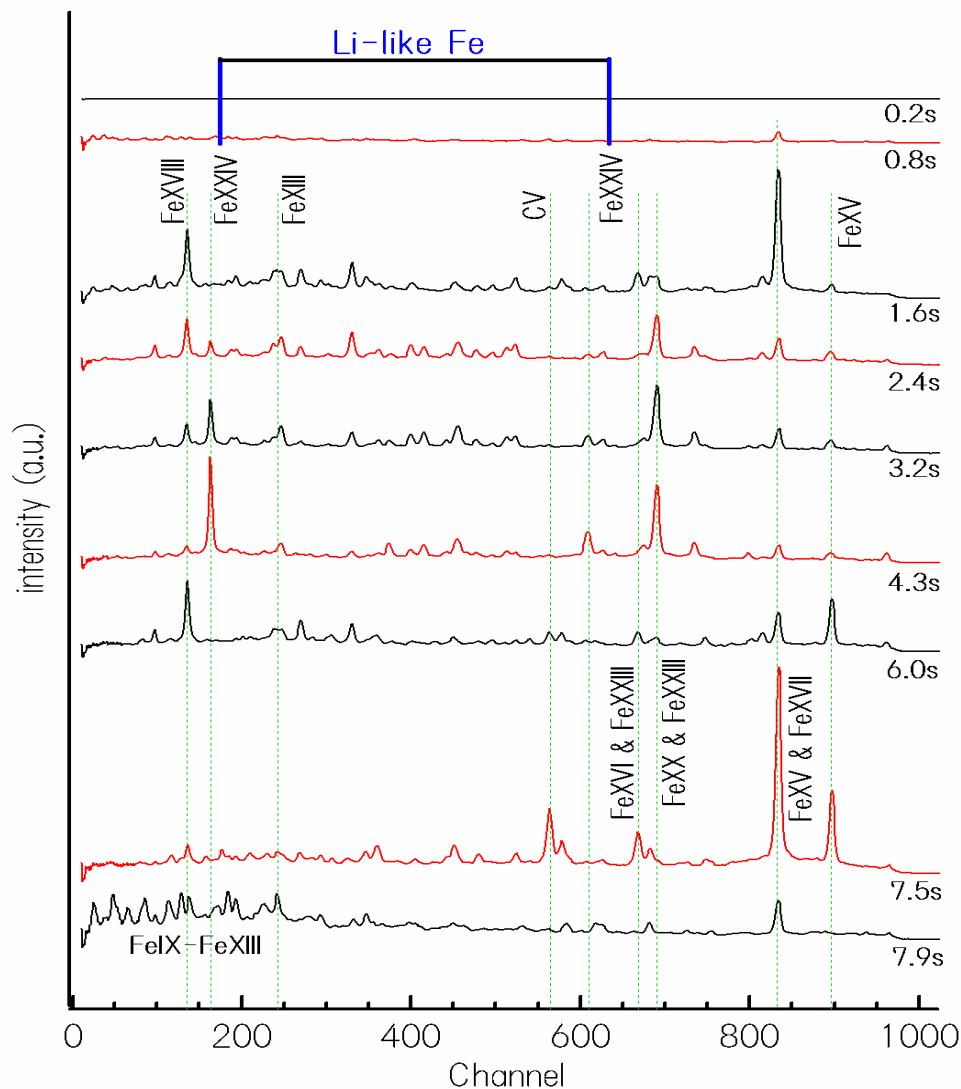
Injection Time: 1.0s

### **Plasma Heating** :

NBI (neutral beam injection)

ECH (electron cyclotron resonance heating)

ICRF (ion cyclotron range-of-frequency)?



### Spectrometer:

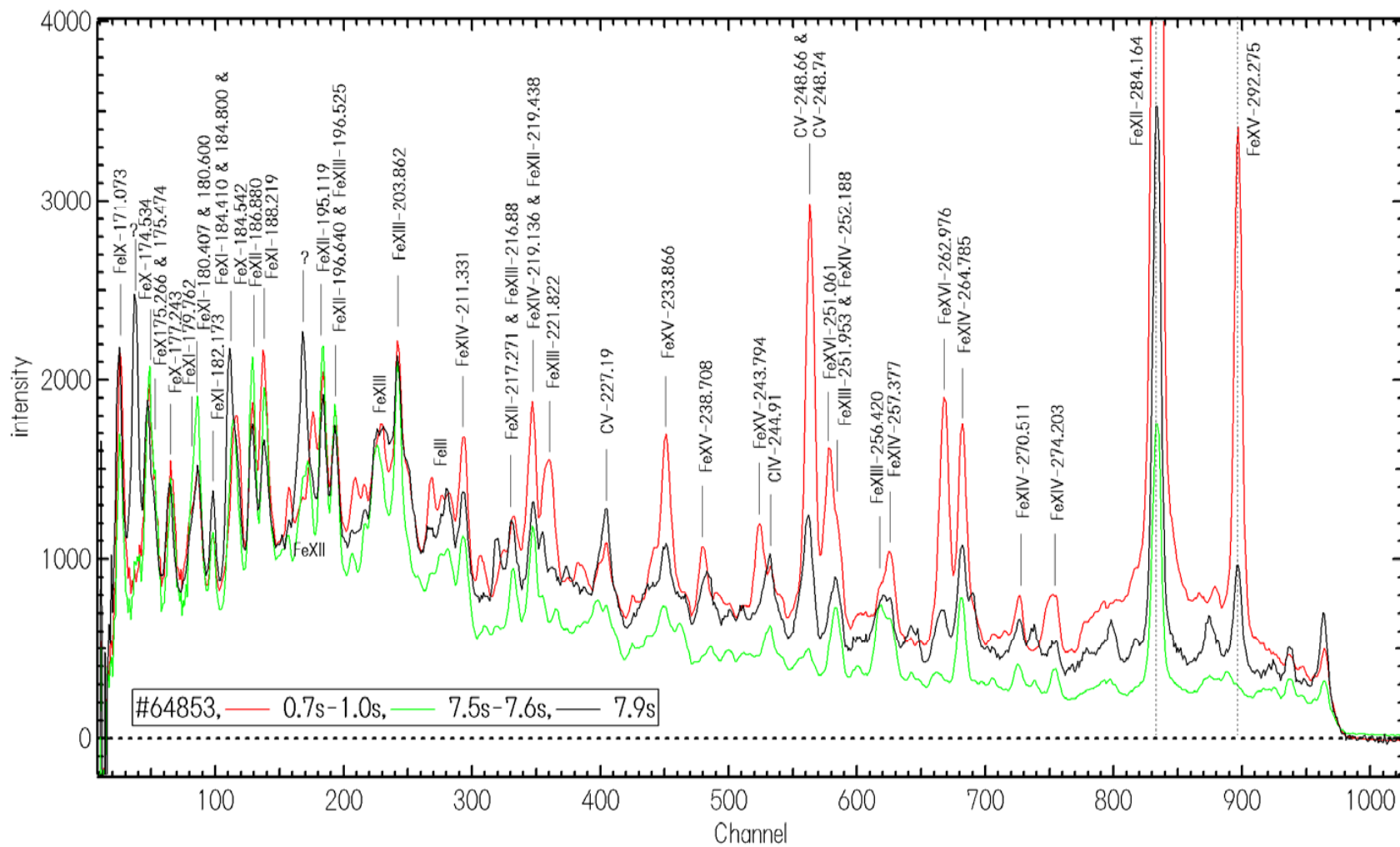
Time resolution: **0.1s**  
 Wavelength resolution: **0.13Å/ch**  
 Total Frame: **80**  
 Direction angle: **-0.1degree**  
 Measurement band: **~165-300Å**

**Highest  
Temperature ?**

### Timing of Heating:

ECH82.7: **0.0-1.0s**, ECH84: **5.5-6.0s**  
 NBI#1: **7.0-11.0s**, NBI#2: **1.0-4.5s**,  
 NBI#3: **4.0-7.0s**  
 ICRF: ---

### Spectra from Low temperature Plasma



# EBIT experiment for Fe M-shell transitions

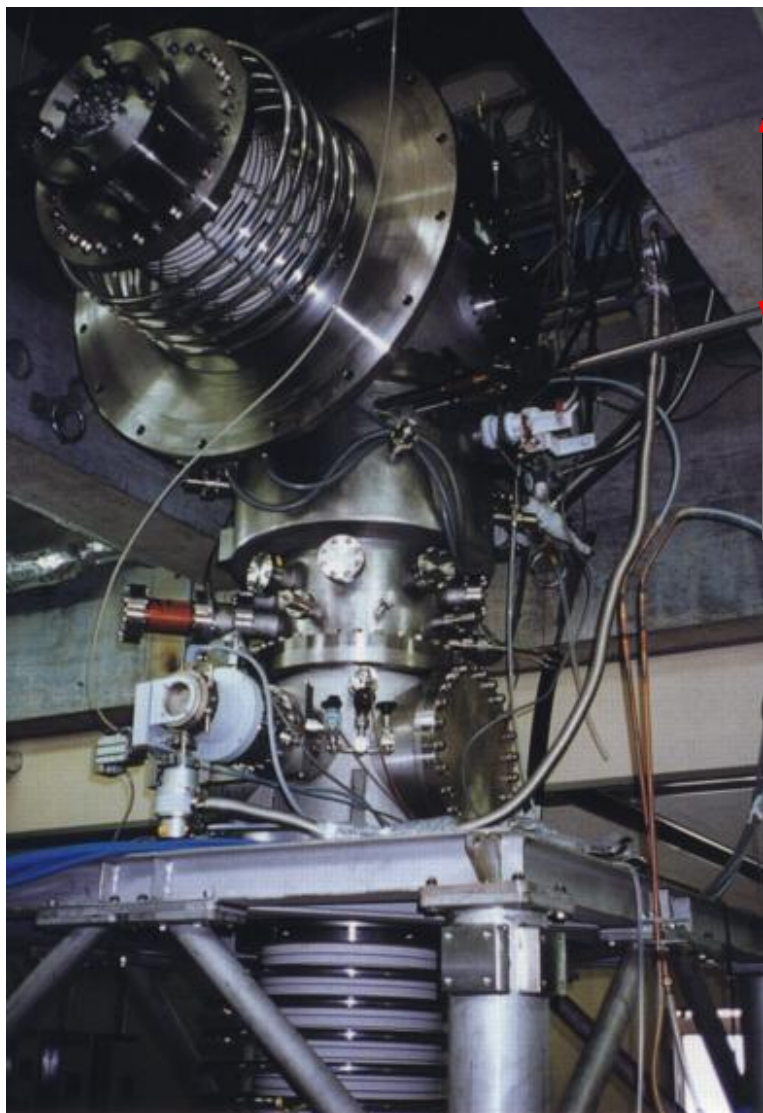
## *CO(ronal e)BIT\* project*

- $N_e: 10^{12} \text{ cm}^{-3}$
- $N_i: 10^{8-9} \text{ cm}^{-3}$
- $E_e: \text{mono-energetic } 1\text{-}100 \text{ keV}$

Electron energy  $\leftrightarrow$  ionization stage

\*: kobito = dwarf

## Solar and LHD (Large Helical Device) Plasma Diagnostics in EUV



~~ANY ion can be produced !!!  
(any charge state, any element)~~

### Tokyo-EBIT

at The Univ. of Electro-Communications

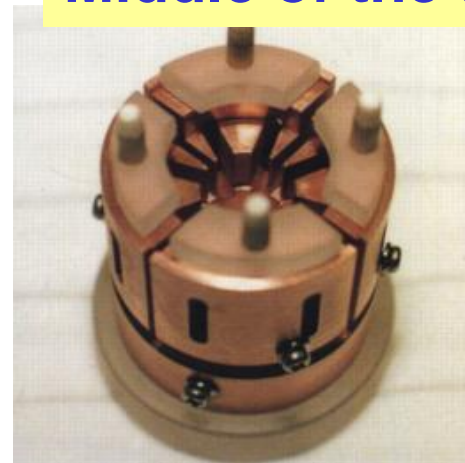
Max. Ee: 200 keV (achieved)

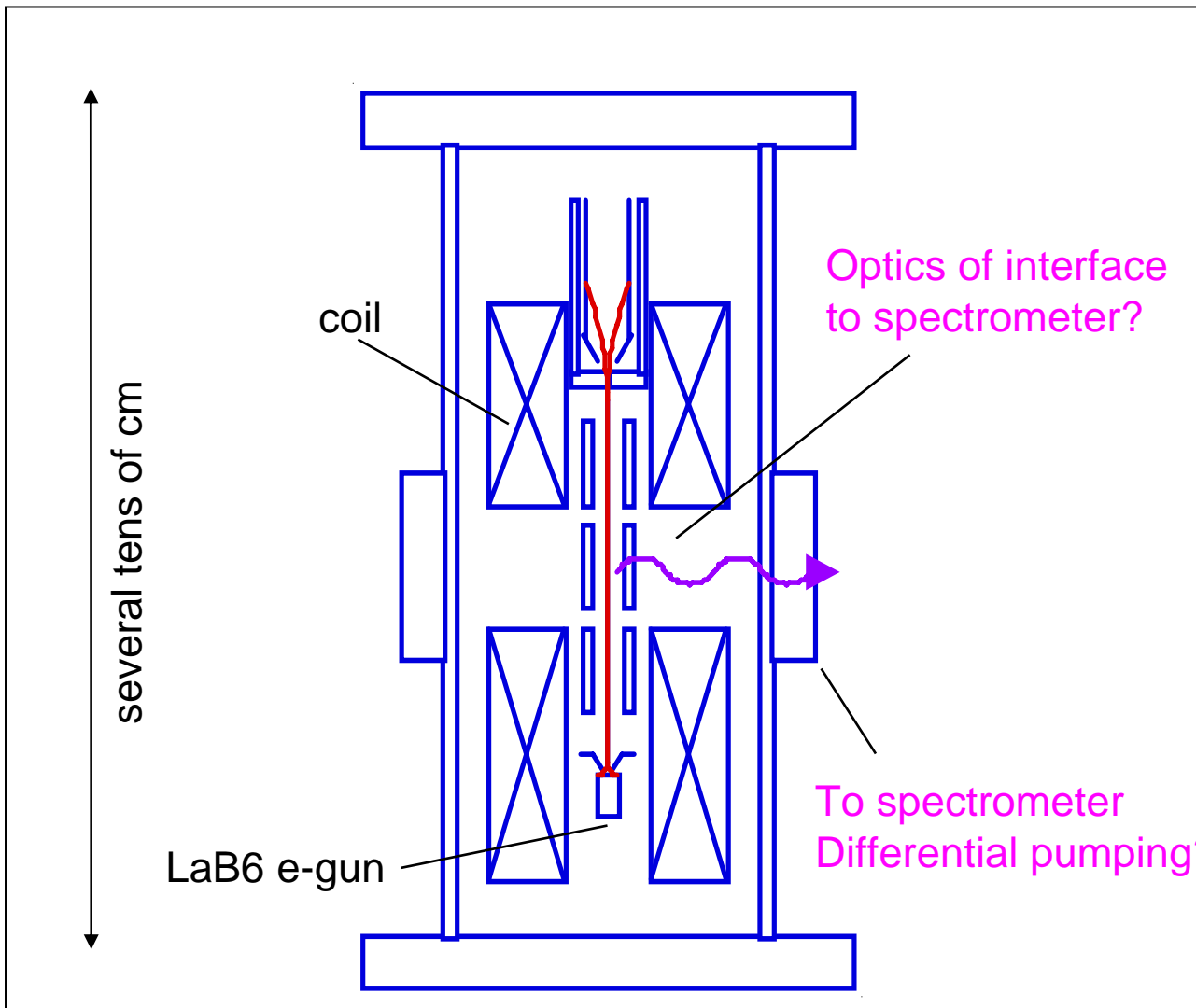
Max. Ie: 330 mA (achieved)

Ion trap



Middle of the trap





# CoBIT (Coronal eBIT)

$E_e$ : 0.1-1 keV  
 $I_e$ : >10mA  
 $B \sim 0.1T$   
 No cooling  
 or LN<sub>2</sub> cooled